Expression of Rat Aspartyl-tRNA Synthetase in Saccharomyces cerevisiae

Fabrice Agou, Jean-Pierre Waller, Marc Mirande

THE JOURNAL OF BIOLOGICAL CHEMISTRY
Vol. 271, No. 46, Issue of November 15, pp. 29295–29303, 1996

Printed in U.S.A.

Expression of Rat Aspartyl-tRNA Synthetase in *Saccharomyces cerevisiae*

ROLE OF THE NH_2-TERMINAL POLYPEPTIDE EXTENSION ON ENZYME ACTIVITY AND STABILITY*

(Received for publication, March 12, 1996, and in revised form, August 13, 1996)

Fabrice Agou‡, Jean-Pierre Waller, and Marc Mirande§

From the Laboratoire d'Enzymologie et Biochimie Structurales, CNRS, Gif sur Yvette, France

Cytoplasmic aspartyl-tRNA synthetase from mammals is one of the components of a multienzyme complex comprising nine synthetase activities. The presence of an amino-terminal extension composed of about 40 residues is a characteristic of the eukaryotic enzyme. We report here the expression in the yeast *Saccharomyces cerevisiae* of a native form of rat aspartyl-tRNA synthetase and of two truncated derivatives lacking 20 or 36 amino acid residues from their amino-terminal polypeptide extension. The three recombinant enzyme species were purified to homogeneity. They behave as α_2 dimers and display catalytic parameters in the tRNA aminoacylation reaction identical to those determined for the native, complex-associated form of aspartyl-tRNA synthetase isolated from rat liver. Because the dimer dissociation constant of rat AspRS is much higher than that of its bacterial and yeast counterparts, we could establish a direct correlation between dissociation of the dimer and inactivation of the enzyme. Our results clearly show that the monomer is devoid of amino acid activation and tRNA aminoacylation activities, indicating that dimerization is essential to confer an active conformation on the catalytic site. The two NH_2-terminal truncated derivatives were fully active, but proved to be more unstable than the recombinant native enzyme, suggesting that the polypeptide extension fulfills structural rather than catalytic requirements.

Aminoacyl-tRNA synthetases are essential enzymes that catalyze a key step during the process of protein biosynthesis: activation of a specific amino acid and the charging of the cognate tRNA (1). On the basis of the comparison of the primary structures of the 20 enzymes from *Escherichia coli*, it was shown that this family is composed of two phylogenetically distinct protein groups harboring mutually exclusive sets of conserved sequence motifs (2). Accordingly, the topological arrangement of the active site domain, as well as the mode of tRNA:enzyme recognition, are essentially different for these two enzyme classes (3). Class I enzymes are characterized by the two consensus sequences HIGH and KMSKS, which are arranged within a structural fold of the Rossmann type: a six-stranded parallel β-sheet. On the other hand, the structural base for the catalytic domain of class II enzymes is a six-stranded anti-parallel β-sheet that supports three conserved sequence motifs.

Crystallographic studies designate motifs 2 and 3 of class II aminoacyl-tRNA synthetases as essential pieces of their active site (4–9). This was confirmed by site-directed mutagenesis of presumed key amino acids within these conserved sequences (4, 10–12). Motif 1 was originally described as a prominent structural element building the subunit interface of class II enzymes that form α_2 dimers. Because the corresponding residues belong to a long α-helix and a β-strand located at the dimeric interface, it was first believed that motif 1 is a key element of oligomerization. However, recent data suggest that this motif is predominantly involved in stabilizing the conformation of the active sites of the two monomers and participates in intersubunit communication (9, 13, 14). Furthermore, a canonical motif 1 was also identified in two monomeric class II enzymes: Ala-tRNA synthetase from yeast, insect, or human (15) and Phe-tRNA synthetase from yeast mitochondria (16). Therefore, the conserved structural motif that builds the dimeric interface of class II synthetases is likely to be indispensable, but not sufficient for oligomerization.

Aspartyl-tRNA synthetase (AspRS)[1] is one of the well known class II enzymes (4, 17). The primary structures of 12 AspRS enzymes, from archaebacteria (*Pyrococcus sp.*), eubacteria (*E. coli*, *Haemophilus influenzae*, *Thermus thermophilus*, *Mycobacterium leprae*, *Mycoplasma genitalium*, *Mycoplasma capricolum*, mitochondria from *Saccharomyces cerevisiae*) and eukaryotes (*Caenorhabditis elegans*, cytoplasma from *S. cerevisiae*, *Rattus norvegicus*, *Homo sapiens*) have been determined through gene cloning, and the 3-D structures of a prokaryotic (*T. thermophilus*) and an eukaryotic (*S. cerevisiae*) AspRS resolved. One particular feature that distinguishes mammalian AspRS from all other known AspRS species concerns its assembly within a multienzyme complex comprising eight other aminoacyl-tRNA synthetases: glutamyl-, prolyl-, isoleucyl-, leucyl-, methionyl, glutaminyl-, lysyl-, and arginyl-tRNA synthetase (18). Rat (19) and human (20) AspRS display an NH_2-terminal polypeptide extension that could fold into an amphiphilic α-helix (21). This extension is dispensable for the catalytic activity of the enzyme (22, 23), but it was shown *in vivo* that the association of AspRS to the complex is abolished by the removal of 34 residues from the NH_2-terminal extremity of the protein (22).

To investigate *in vitro* the functional properties of rat AspRS and of genetically engineered mutant enzymes, large amounts of purified proteins are required. The availability of the cloned

* This work was supported in part by grants from CNRS, the Fondation pour la Recherche Médicale, the Association pour la Recherche sur le Cancer, and the Agence Nationale de Recherches sur le SIDA. The costs of publication of this article were defrayed in part by the payment of page charges. This article must therefore be hereby marked "*advertisement*" in accordance with 18 U.S.C. Section 1734 solely to indicate this fact.

‡ Fellow of the Ligue Nationale contre le Cancer.

§ To whom correspondence should be addressed. Tel.: 33-1-69-82-35-05; Fax: 33-1-69-82-31-29; E-mail: marc.mirande@lebs.cnrs-gif.fr.

[1] The abbreviations used are: AspRS, aspartyl-tRNA synthetase; rAspRS, recombinant native AspRS; Cx-AspRS, complex-associated AspRS; BSA, bovine serum albumin; DTE, dithioerythritol; AMPPCP, adenosine 5'-(β,γ-methylene)triphosphate.

cDNA provided the opportunity to construct an overproducing strain, to isolate rat AspRS species in a cellular background precluding its association with the other components of the multisynthetase complex, to analyze the catalytic activity as well as the stability of rat AspRS species isolated as free enzymes. In this paper, taking advantage of the high dimer dissociation constant of rat AspRS as compared with its bacterial and yeast counterparts, we also demonstrate that dimerization of a class II synthetase is absolutely required for amino acid activation as well as tRNA aminoacylation.

EXPERIMENTAL PROCEDURES

Strains and Plasmids—M13mp9, the yeast shuttle vectors pYeDP1/8-10 and pYeDP60 (Ref. 24; gift from D. Pompon, Centre de Génétique Moléculaire, Gif sur Yvette, France), and their derivatives were propagated in *E. coli* JM101Tr (Δ(*lac-pro*) *supE thi rec*A56 *srl-300*::Tn*10* F′(*traD36 proAB lacI*^{q} *lacZ*Δ*M15*)). The haploid *S. cerevisiae* strain W303-1B (*MATα leu2 his3 trp1 ura3 ade2 can*^{R} *cyr*$^+$) was provided by D. Pompon.

General Recombinant DNA Techniques—Restriction endonucleases and DNA modifying enzymes were purchased from Boehringer Mannheim or Perkin-Elmer. Radionucleotides were from Amersham. General recombinant DNA manipulations were carried out according to standard procedures (25). Nucleotide sequences were determined by the dideoxynucleotide chain termination method (26). All constructions were confirmed by DNA sequencing. Polymerase chain reaction experiments were performed with 6.6 ng of plasmid DNA, 100 pmol of oligonucleotide primers, and 2.5 units of *Taq* DNA polymerase, in a Perkin-Elmer thermocycler.

Enzymatic Assays—Initial rates of tRNA aminoacylation were measured at 25 °C, unless otherwise stated, in 0.1 ml of 20 mM imidazole-HCl buffer (pH 7.5), 150 mM KCl, 0.5 mM DTE (1, 4-dithioerythritol), 5 mM $MgCl_2$, 3 mM ATP, 60 μM ^{14}C-labeled aspartic acid (Amersham, 50 Ci/mol), and saturating amounts of partially purified beef liver tRNA. The incubation mixture contained catalytic amounts of enzymes appropriately diluted in 10 mM Tris-HCl (pH 7.5), 10 mM β-mercaptoethanol, 20% glycerol, containing bovine serum albumin at 4 mg/ml. One unit of AspRS activity is the amount of enzyme producing 1 nmol of aspartyl-tRNA/min, at 25 °C. Specific activities of purified enzymes were calculated with protein concentrations determined by using absorption coefficients of 0.41, 0.38, and 0.39 A_{280} units·mg^{-1}·cm^2 for rAspRS (the recombinant native AspRS) AspRS-ΔN36 (rAspRS with a deletion of 36 NH_2-terminal residues) and AspRS-ΔN20 (deletion of 20 NH_2-terminal residues), respectively. For the determination of K_m values for tRNA, $tRNA^{Asp}$ concentrations of 0.022–6.6 μM were used, as determined from the aspartyl-acceptance of the tRNA preparation (148 pmol of [^{14}C]aspartic acid/A_{260} unit). Michaelis parameters were obtained by nonlinear regression of the theoretical Michaelis equation to the experimental curve using the KaleidaGraph 3.0.4 software (Abelbeck Software).

The isotopic [^{32}P]PP_i–ATP exchange reaction was assayed at 25 °C, unless otherwise stated, in 0.1 ml of 20 mM imidazole-HCl buffer (pH 7.5), 0.1 mM EDTA, 2.5 mM β-mercaptoethanol, 10 mM $MgCl_2$, 2 mM ATP, 2 mM aspartic acid, and 2 mM [^{32}P]PP_i (Amersham, 0.4 Ci/mol). Reaction was initiated by the addition of an appropriate enzyme dilution. One unit of AspRS activity in the exchange reaction is the amount of enzyme producing 1 nmol of ATP/min, at 25 °C.

Construction of the Expression Vector pYeDP60/DRS for Overproduction of Rat AspRS in S. cerevisiae—An *Eco*RI-*Eco*RI cDNA fragment containing the complete coding sequence of the rat AspRS cDNA (19) was cloned into the *Eco*RI site of pYeDP1/8-10 (24) to give pYeDP1/DRS. This plasmid has the yeast 2-μm origin of replication and the *URA3*-selectable marker but displays a poor mitotic stability. A high stability vector, pYeDP60, was derived from pYeDP1/8-2 by insertion of a yeast DNA fragment containing the *ADE2* gene (24). pYeDP1/8-2 is identical to pYeDP1/8-10 except for the presence of a polylinker in the opposite orientation. To insert the rat AspRS cDNA into pYeDP60, we took advantage of the high efficiency of homologous recombination in yeast. The yeast strain W303-1B was cotransformed with a *Cla*I fragment from pYeDP1/DRS containing the GAL10-CYC1 promoter, the rat AspRS cDNA, and part of the phosphoglycerate kinase terminator, and with pYeDP60 digested with *Bam*HI and *Eco*RI, located in the polylinker region between the GAL10-CYC1 promoter and the phosphoglycerate kinase terminator. Ura$^+$ and Ade$^+$ transformants resulted from recombination events between homologous regions of the two fragments.

Construction of pYeDP60/DRS-ΔN36—The *Bam*HI-*Eco*RI fragment from M13mp9/DRS-ΔN (22) was introduced into pYeDP60 digested with *Bam*HI and *Eco*RI to give pYeDP60/DRS-ΔN36ΔMet. The coding region of rat AspRS started at residue Ser^{37}. The NH_2-terminal sequence MSLDP was provided by insertion of the two complementary oligonucleotides 5′-GATCATAATGTCTCTG-3′ and 3′-TATTACAGAGACCTAG-5′ into the unique *Bam*HI site of pYeDP60/DRS-ΔN36ΔMet to give pYeDP60/DRS-ΔN36.

Construction of pYeDP60/DRS-ΔN20—We produced a DNA fragment by amplification of M13mp9/DRS1 between the oligonucleotides 5′-GGGATCCTTCTCGAGTATGATACAATCACAAG-3′ (F01) and DRS666IC (22). This corresponds to DRS1 cDNA over positions 101–666 and allows the insertion of a *Xho*I site in the coding sequence of rat AspRS. The amplified fragment was digested with *Bam*HI and *Hpa*I and ligated into M13mp9/DRS1 digested with *Bam*HI and *Hpa*I to give M13mp9/DRSΔΔN. The linkers L02, made of 5′-GATCCATAATGCCCAGCGCCAACGCCCT-3′ and 3′-GTATTACGGGTCGCGGTTGCGGGAGATC-5′, and L04, made of 5′-CTAGAAAGGGTGTC-3′ and 3′-TTTCCCACAGAGCT-5′, were inserted into M13mp9/DRSΔΔN digested with *Bam*HI and *Xho*I. The resulting plasmid M13mp9/DRSΔ11-30 was digested with *Bam*HI and *Eco*RI and the DNA insert cloned into pYeDP60 digested by *Bam*HI and *Eco*RI.

Expression of Rat AspRS in S. cerevisiae—The yeast cell W303-1B was transformed by the lithium chloride method (27). Ura$^+$ and Ade$^+$ transformants were selected on plates containing 0.7% yeast nitrogen base (Difco), 0.1% casamino acids (Difco), 5% D-glucose, and 20 μg/ml L-tryptophan. Expression of rat AspRS was induced by growth on plates containing 2% D-galactose instead of glucose. Cells were grown at 28 °C in 50 ml of YPGal (0.5% yeast extract (Difco), 0.5% Bacto-peptone (Difco), 2% D-galactose) to a cell density corresponding to $A_{600} \sim 1$–2. All subsequent steps were performed at 4 °C. Cells were harvested; washed twice with 100 mM Tris-HCl (pH 8.0), 10 mM $MgCl_2$, 1 mM EDTA, 1 mM DTE; resuspended in 0.3 ml of 25 mM potassium phosphate (pH 7.5), 10% glycerol, 1 mM DTE, 1 mM EDTA containing 1 mM diisopropyl fluorophosphate, 12 μg/ml pepstatin A, and 6 μg/ml leupeptin (Protein Research Foundation, Osaka, Japan); and broken with glass beads (200 μl, 0.45–0.50 mm) by vigorous shaking (0.5 min, 10 times). After centrifugation for 15 min at 10,000 × *g*, the supernatant was assayed for AspRS activity by the aminoacylation of tRNA. Protein concentration was determined according to Ref. 28.

Purification of rAspRS from a S. cerevisiae-overproducing Strain—Yeast cells W303-1B:pYeDP60/DRS that express the native recombinant AspRS were grown at 28 °C in 3 liters of YPGal to an absorbance of $A_{600} \sim 8$. Cells were washed, resuspended in 40 ml of extraction buffer containing the protease inhibitors, as described above, and lysed in an Eaton press at 5000 p.s.i. The lysate was diluted 2.5-fold with extraction buffer supplemented with 1 mM diisopropyl fluorophosphate, and centrifuged at 10,000 × *g* for 30 min to remove cell debris.

All chromatographic steps were performed at 4 °C. The suspension was applied to a S Sepharose FF column (Pharmacia, 2.5 × 9.4 cm) equilibrated in 25 mM potassium phosphate (pH 7.5), 10% glycerol, 1 mM EDTA, 1 mM DTE and eluted with a 1500-ml linear gradient of potassium phosphate from 25 to 300 mM (pH 7.5) containing the same additives. Fractions containing rat AspRS (eluted at 75 mM) were fractionated further on a Q Sepharose FF column (Pharmacia, 1.1 × 10.5 cm) equilibrated in 75 mM potassium phosphate, pH 7.5, 10% glycerol, 1 mM DTE and eluted with a 300-ml linear gradient of potassium phosphate from 75 to 300 mM (pH 7.5). Fractions containing AspRS activity (eluted at 110 mM) were pooled, diluted 5-fold with 10% glycerol and 1 mM DTE, and applied to a 1.1 × 8.5-cm column of tRNA-Sepharose (29) equilibrated in 25 mM potassium phosphate (pH 7.5), 10% glycerol, 1 mM DTE. The column was eluted with a 200-ml linear gradient of potassium phosphate from 25 mM to 200 mM (pH 7.5). Fractions containing AspRS activity (eluted at 70 mM) were pooled; concentrated by vacuum dialysis; dialyzed against 25 mM potassium phosphate (pH 7.5), 1 mM DTE, 50% glycerol; and stored at −20 °C. The homogeneity of the enzyme preparation was checked by SDS-polyacrylamide gel electrophoresis (30) and by NH_2-terminal amino acid sequence analysis. Automated Edman degradations were performed by J.-P. Le Caer (Laboratoire de Physiologie Nerveuse, Gif sur Yvette, France) using an Applied Biosystems model 470A sequencer.

Purification of the NH_2-terminal Truncated Forms of Rat AspRS Produced in Yeast—The purification of the mutant enzymes was conducted as described for rAspRS, except that all buffers contained 20% glycerol to prevent enzyme inactivation. The NH_2-terminal deletions modify the global net charge of the protein: −1 for AspRS-ΔN36 and +2 for AspRS-ΔN20. Accordingly, they were eluted on S Sepharose FF, Q Sepharose FF, and tRNA-Sepharose at phosphate concentrations of 70 and 135 mM, 125 and 100 mM, and 60 and 105 mM, respectively, for

AspRS-ΔN36 and AspRS-ΔN20.

Analytical Gel Filtration—The apparent native molecular mass of the AspRS species was determined at room temperature by gel filtration on a Superose 12 HR 10/30 (Pharmacia) column equilibrated in 50 mM potassium phosphate (pH 7.5), 10 mM β-mercaptoethanol, containing 5 or 20% glycerol, and developed at a flow rate of 0.2 ml·min^{-1}. All samples (100 μg of protein) were loaded in 0.2 ml. The calibration curve was established by using bovine serum albumin, thyroglobulin, and soybean trypsin inhibitor as marker proteins. For a particular protein, its elution was described in term of the corresponding K_{av} value. $K_{av} = (V_e - V_0)/(V_t - V_0)$, where V_e is the elution volume of the particular molecule, V_0 the void volume of the column, and V_t the total bed volume. V_0 and V_t were determined with thyroglobulin (670 kDa) and DTE (154 Da), respectively.

Analytical Ultracentrifugation—Sedimentation equilibrium experiments were performed in a Beckman Optima XL-A analytical ultracentrifuge, using an An-60 Ti rotor and a double-sector cell of 12 mm path length. The solution column was 0.1–0.2 cm; data were collected with a spacing of 0.001 cm. Equilibrium was verified from the superimposition of duplicate scans recorded at 4-h intervals. The experimental data were first fitted to a model for a single homogeneous species following the equation below.

$$c(r) = c(r_{ref})\exp\{[M(1 - \bar{v}\rho)\omega^2/2RT](r^2 - r_{ref}^2)\} \qquad \text{(Eq. 1)}$$

$c(r)$ is the concentration of the protein at radial position r, $c(r_{ref})$ is the concentration of the protein at an arbitrary reference distance r_{ref}, M is the molecular weight, $\bar{v}$ the partial specific volume of the solute, ρ is the density of the solvent, ω is the angular velocity, and R and T are the molar gas constant and the absolute temperature, respectively. The partial specific volume was calculated from the amino acid composition of the protein sample, and the density of the buffers was determined from published tables (31). Where the experimentally determined M did not converge on the true mass of the samples (56,960, 54,650, and 53,510 for rAspRS, AspRS-ΔN20, and AspRS-ΔN36, respectively), the data were fitted to a monomer-i-mer equilibrium, according to Equation 2, where c_i are the concentrations of the i-mer.

$$c(r) = \sum_i c_i(r_{ref})\exp\{[iM(1 - \bar{v}\rho)\omega^2/2RT](r^2 - r_{ref}^2)\} \qquad \text{(Eq. 2)}$$

In all cases, since inclusion of a second virial coefficient gave no improvement of the fit, an ideal component system was considered.

RESULTS

Expression of Rat AspRS in Yeast—We first tried to express and purify rat AspRS from a bacterial overproducing strain. Whereas aminoacylation activities could be readily measured in crude extracts from *E. coli* transformed with various expression vectors (19), rat AspRS proved to be very unstable during subsequent chromatographic steps, leading to a poorly active enzyme preparation. Expression of heterologous genes in the yeast *S. cerevisiae* has proved to be useful as an alternative approach (32). In order to obtain high yields of recombinant proteins, we used a multicopy shuttle vector with a high mitotic stability. The pYeDP60 vector propagates in yeast grown in rich medium, allowing to obtain a high cell density (24). Foreign proteins are expressed under the control of the hybrid GAL10-CYC1 promoter, which is activated in galactose-containing media and repressed in the presence of glucose.

The cDNA encoding rat AspRS was introduced into pYeDP60 and the recombinant plasmid used to transform the yeast strain W303-1B grown in the presence of glucose. To test for the level of expression and the putative toxicity of native rat AspRS in yeast, transformed cells were grown in rich medium containing galactose (YPGal). As shown in Fig. 1, a polypeptide with an apparent molecular mass of 57 kDa, identical to that of the AspRS component of the multisynthetase complex, is specifically detected in a crude extract from yeast cells carrying the recombinant plasmid pYeDP60/DRS. By Western blot analysis, only this polypeptide is detected with antibodies raised against the AspRS component from the sheep liver complex (data not shown). In addition, AspRS activity was assayed in the corresponding crude extracts by the aminoacylation of beef tRNA. In these conditions, W303-1B transformed with pYeDP60/DRS overproduced AspRS activity 80-fold, as compared with the endogenous yeast AspRS activity detected with the control strain. Since the mock and overproducing strains grew at approximately the same rate, no deleterious effect resulted from the expression of rat AspRS in *S. cerevisiae*.

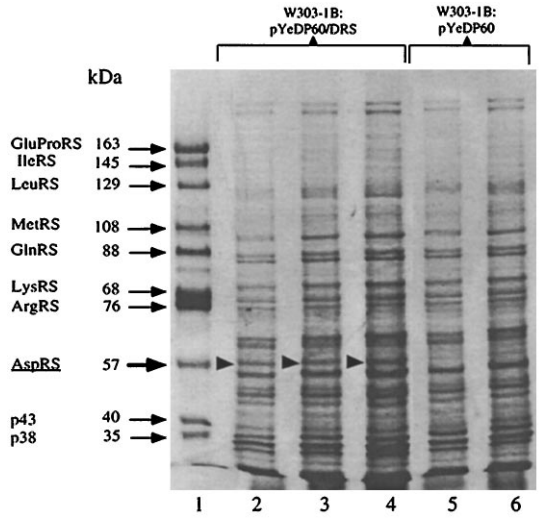

FIG. 1. **Expression of rat AspRS in yeast.** Crude extract from yeast cell W303-1B transformed with pYeDP60 (*lanes 5* and *6*) or with pYeDP60/DRS (*lanes 2–4*) were analyzed by SDS-PAGE with a 8% gel, by loading 20 μg (*lanes 2* and *5*), 40 μg (*lanes 3* and *6*), or 60 μg (*lane 4*) of total protein. The polypeptide specifically expressed in strain W303-1B:pYeDP60/DRS is indicated by an *arrowhead*. The recombinant protein accounts for approximately 3% of cell proteins. The purified multisynthetase complex from rat is shown at *left* (*lane 1*). The identity and molecular mass of the polypeptide components of the complex are marked, and the AspRS component is *underlined*. The gel was stained with Coomassie Blue.

Purification of Rat AspRS Produced in Yeast—The recombinant AspRS (rAspRS) was purified to homogeneity from a culture of W303-1B:pYeDP60/DRS grown in the presence of galactose as the carbon source. Three chromatographic steps on S Sepharose FF, Q Sepharose FF, and tRNA-Sepharose were used as described under "Experimental Procedures." At each step, rAspRS was eluted as a single, symmetrical peak. This purification procedure yields 15 mg of homogeneous rAspRS/32 g of cell pellet, with a global recovery of 38% of AspRS activity (Table I). The purified rAspRS has an apparent molecular mass of 57 kDa identical to that of the AspRS component of the multisynthetase complex from rat and was judged to be at least 95% homogeneous according to SDS-PAGE analysis (Fig. 2, *lanes 2* and *5*). Its specific activity of 380 units/mg indicates that the rat enzyme produced in yeast is fully active. Indeed, in the same assay conditions, AspRS activity from the purified complex from rat is of 28 units/mg of complex (33), that is 350 units/mg of the AspRS component, taking into account the presence of 1 mol of AspRS (α_2, 114 kDa)/mol of complex (1,450 kDa). To assess the integrity and the homogeneity of the enzyme preparation, 25 cycles of automatic Edman degradations were performed. A single amino acid sequence was obtained, corresponding to residues 2–26 of the cDNA-encoded protein. The removal of the initiating methionine when the second amino acid is a proline is in accordance with the rules of post-translational modification in yeast (34).

Expression and Purification of NH_2-terminal Truncated Derivatives of Rat AspRS—Two derivatives of rat AspRS were constructed in pYeDP60, expressed in yeast, and purified to homogeneity. The first of these derivatives, AspRS-ΔN36, previously expressed in cultured Chinese hamster ovary cells, was

TABLE I
Purification of native AspRS and of NH_2-terminal truncated derivatives

Purification step	Protein	Total activity[a]	Specific activity	Yield	Relative purification factor
	mg	*units*	*units/mg*	*%*	
Purification of rAspRS					
Crude extract	1350	14,850	11	100	1
S-Sepharose FF	47	10,998	234	74	21
Q-Sepharose FF	18	6120	340	41	31
tRNA-Sepharose	15	5700	380	38	35
Purification of AspRS-ΔN36					
Crude extract	1633	19,000	11	100	1
S-Sepharose FF	62	15,760	250	83	23
Q-Sepharose FF	28	10,363	366	55	34
tRNA-Sepharose	11	4795	410	25	38
Purification of AspRS-ΔN20					
Crude extract	1190	11,892	10	100	1
S-Sepharose FF		8710		73	
Q-Sepharose FF		5850		49	
tRNA-Sepharose	13	5150	395	43	39

[a] One unit of activity corresponds to the formation of 1 nmol of aminoacyl-tRNA/min at 25 °C in the standard assay conditions.

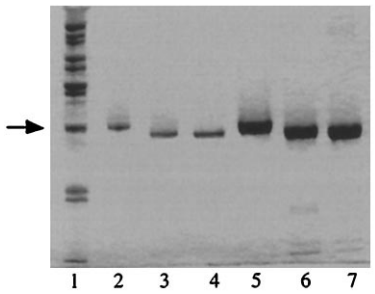

FIG. 2. **SDS-PAGE analysis of the purified AspRS species produced in yeast.** The purified enzyme preparations (0.2 μg of protein in *lanes 2–4*; 2 μg of protein in *lanes 5–7*) rAspRS (57 kDa; *lanes 2* and *5*), AspRS-ΔN20 (54.6 kDa; *lanes 3* and *6*), and AspRS-ΔN36 (53.5 kDa; *lanes 4* and *7*) were analyzed on a 10% polyacrylamide gel. The rat multisynthetase complex (*lane 1*) was used as size marker; the AspRS component is indicated by an *arrow*.

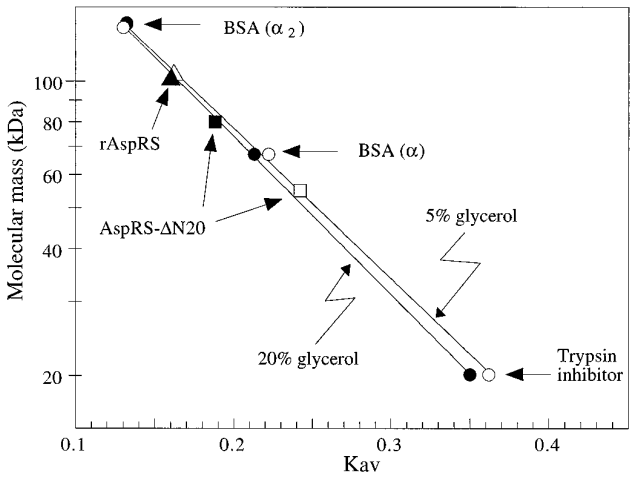

FIG. 3. **Superose 12 chromatography of rAspRS and AspRS-ΔN20.** Gel filtration was conducted as described under "Experimental Procedures," in the presence of 20% (●, ■, ▲) or 5% (○, □, △) glycerol in the equilibration buffer. The apparent, native molecular masses of rAspRS (▲, △) and AspRS-ΔN20 (■, □) were estimated to 100 kDa (▲) and 80 kDa (■) in the presence of 20% glycerol or 100 kDa (△) and 55 kDa (□) with 5% glycerol.

already described (22). Another NH_2-terminal truncated form of rat AspRS was constructed. The AspRS-ΔN20 derivative has an amino acid sequence identical to that of the native enzyme, except for a 20-amino acid deletion from Gln^{11} to Gly^{30}, corresponding to the precise removal of a putative amphipathic α-helix (20). The level of expression of AspRS-ΔN20 and AspRS-ΔN36 is similar to that of rAspRS, as judged by Western blotting and activity measurement. The truncated AspRS derivatives were purified as described for rAspRS, except that all buffers were supplemented with 20% glycerol instead of 10%. The use of higher glycerol concentrations was found to be required to preserve AspRS activity of the mutant enzymes, which are very sensitive to dissociation, as shown below. The two truncated enzymes are recovered with yields comparable with that obtained for the native enzyme, and the purified preparations display similar specific activities (Table I). This result already demonstrates that the NH_2-terminal extension is dispensable for enzyme activity. The native and truncated forms rAspRS, AspRS-ΔN20, and AspRS-ΔN36 display electrophoretic mobilities in accordance with their calculated masses of 57, 54.6, and 53.5 kDa, respectively (Fig. 2).

Quaternary Structure of AspRS and Dissociation Equilibrium—The molecular masses of the rat AspRS species produced in yeast were determined by gel filtration on Superose 12 (Fig. 3). The molecular mass standards included the monomer (67 kDa) and dimer (134 kDa) of bovine serum albumin and soybean trypsin inhibitor (20 kDa). An apparent native molecular mass of 100 kDa was deduced for rAspRS, when analyzed in the presence of either 5% or 20% glycerol in the equilibration buffer. This value reasonably compares with a theoretical mass of 114 kDa for a dimer. The behavior of the truncated species AspRS-ΔN20 and AspRS-ΔN36 is very sensitive to the glycerol concentration of the buffer (Fig. 3). The molecular masses of 80 kDa and 85 kDa observed for the ΔN20 and ΔN36 species, respectively, in the presence of 20% glycerol, indicate a tendency to dissociation of the dimers. In the presence of 5% glycerol, molecular masses of 55 and 57 kDa are determined and no AspRS activity can be recovered. These results suggested that the truncated forms of AspRS are dimers that readily dissociate and inactivate in the presence of low glycerol concentrations.

The stability and dissociation of the various AspRS species were examined by sedimentation equilibrium analysis. The oligomeric structure of the enzyme preparations was determined under different experimental conditions (Table II, Fig. 4). The influence of the glycerol on the oligomeric structure of AspRS was first analyzed. The native rAspRS behaves as a dimer in 50 mM Tris-HCl, pH 7.5, containing either 20% or 5% glycerol. By contrast, AspRS-ΔN36 has a tendency to dissociate, even in the presence of 20% glycerol, and forms large aggregates at 20 °C. These high molecular weight species are mainly due to the instability of the monomer. Lowering the temperature to 4 °C stabilizes the monomer, thus preventing its irreversible aggregation.

TABLE II
Summary of sedimentation equilibrium experiments with recombinant native and truncated forms of rat AspRS

Buffer[a]	Temperature	Detection wavelength	Initial protein concentration	Speed	Monomer-oligomer equilibrium[b]	
					Distribution of molecular species	Deduced M_r of the monomer
	°C	*nm*	*mg/ml*	*rpm*	*%*	
rAspRS						
50 mM Tris-HCl, 20% glycerol	20	280	0.5	13,000	100 α_2	56,000
50 mM Tris-HCl, 5% glycerol	20[c]	280	0.5	13,000	100 α_2	57,000
50 mM Tris-HCl, 200 mM KCl	20	280	1.0	15,000	15 α, 85 α_2	55,000
	20[c]	280	0.2	15,000	35 α, 65 α_2	60,000
25 mM potassium phosphate, 200 mM KCl	4	280	0.3	15,000	80 α, 5 α_2, 15 α_4	56,000
	4	220	0.03	15,000	100 α	60,000
AspRS-ΔN36						
50 mM Tris-HCl, 20% glycerol	4	280	0.6	15,000	60 α, 40 α_2	52,000
	4	280	0.2	15,000	80 α, 20 α_2	55,000
	20	280	0.2	15,000	α_n	
50 mM Tris-HCl, 200 mM KCl	20	280	0.2	15,000	α_n	
	4	220	0.05	15,000	α_n	
AspRS-ΔN20						
50 mM Tris-HCl, 200 mM KCl	20	280	0.2	15,000	α_n	
	4[c]	220	0.05	15,000	100 α	52,000
AspRS from *S. cerevisiae*						
50 mM Tris-HCl, 500 mM KCl	4	280	0.5	15,000	100 α_2	63,000

[a] All buffers are adjusted to pH 7.5 and contain 1 mM dithioerythritol.
[b] The data were analyzed as described under "Experimental Procedures" by using Equation 1 or 2. The values that best fit experimental data are indicated, taking into account the presence of various α_i species in solution. α_n indicates that heterogeneous high molecular weight aggregates were formed.
[c] Profiles of protein distribution are shown in Fig. 4.

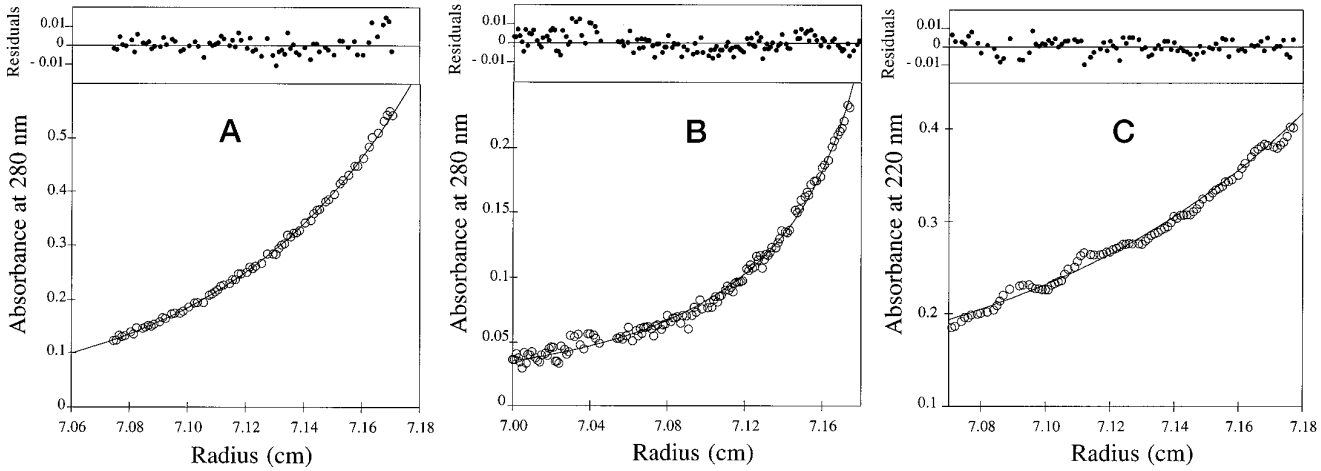

FIG. 4. **Sedimentation equilibrium distribution of rAspRS and AspRS-ΔN20.** Relative concentration of rAspRS (*A* and *B*) or AspRS-ΔN20 (*C*), measured by absorbance at 280 or 220 nm, is plotted as a function of radial distance after sedimentation in conditions of Table II. *A*, rAspRS at 0.5 mg·ml^{-1} in 50 mM Tris-HCl pH 7.5 and 5% glycerol, at 20 °C; *B*, rAspRS at 0.2 mg·ml^{-1} in 50 mM Tris-HCl, pH 7.5, and 200 mM KCl, at 20 °C; *C*, AspRS-ΔN20 at 0.05 mg·ml^{-1} in 50 mM Tris-HCl, pH 7.5, and 200 mM KCl, at 4 °C. Experimental values (*open circles*) were fitted (*curves*) as described under "Experimental Procedures": residuals are indicated above each fit. The best fits were calculated for monodisperse solutes of 114 kDa (*A*) and 52 kDa (*C*), or a monomer-dimer equilibrium (*B*) with the mass of the monomer equal to 60 kDa and a dimer dissociation constant of 0.5×10^{-6} M.

The effect of chaotropic salts on the stability of AspRS dimers was examined (Table II). The addition of KCl to 0.2 M induced partial dissociation of rAspRS and caused AspRS-ΔN36 and AspRS-ΔN20 to aggregate. In the case of AspRS-ΔN20, no aggregation occurs when sedimentation equilibrium analysis is conducted at 4 °C and at low protein concentration, and an homogeneous monomer species is observed (Fig. 4). The AspRS-ΔN36 derivative is more unstable, generating large aggregates in these conditions.

When the distribution of material along the column could be satisfactorily fitted to a model of monomer-dimer equilibrium, dissociation constants of 0.5×10^{-6} M and 5×10^{-6} M were deduced for rAspRS in 200 mM KCl at 20 °C and AspRS-ΔN36 in 20% glycerol at 4 °C, respectively. Following sedimentation analysis of AspRS from *S. cerevisiae* in the presence of up to 500 mM KCl, at 4 °C, the experimental distribution was fitted to a monodisperse solute of 125.5 kDa. This value precisely correlates with the calculated mass of a dimeric species (126.8 kDa). No reversible thermodynamic equilibrium is observed, indicating that the dimer dissociation constant of yeast AspRS is at least 10-fold lower than that of the rat enzyme.

The sedimentation equilibrium data indicate that rat AspRS can be readily dissociated by lowering glycerol concentration, temperature, or protein concentration or by increasing the concentration of chaotropic salts, conditions that do not significantly affect the dimeric yeast enzyme. The NH_2-terminal truncated derivatives show a more pronounced tendency to dissociation. Whereas their dimer dissociation constants at 20 °C are lower than at 4 °C, the truncated monomer species prove to be more unstable at 20 °C than at 4 °C, leading to

TABLE III
Kinetic constants of native rat AspRS and of NH_2-terminal truncated derivatives in the $tRNA^{Asp}$ aminoacylation reaction

Kinetic constant[a]	AspRS-Cx[b]	rAspRS	AspRS-ΔN36	AspRS-ΔN20
K_M $tRNA^{Asp}$ (μM)	0.50 ± 0.05	0.50 ± 0.05	0.6 ± 0.1	0.6 ± 0.1
k_{cat} (s^{-1})	1.0 ± 0.1	1.1 ± 0.1	1.1 ± 0.1	1.1 ± 0.1

[a] The K_M values refer to aspartic acid acceptor tRNA.
[b] Values determined for the AspRS component of the purified multisynthetase complex from rat liver. The k_{cat} value is corrected for the presence of 1 mol of AspRS (α_2, 114 kDa)/mol of complex (1450 kDa).

aggregation and irreversible inactivation, as shown below.

Dissociation of AspRS and Inactivation—Initial rates of rAspRS, AspRS-ΔN36, and AspRS-ΔN20 in the $tRNA^{Asp}$ aminoacylation reaction were determined in conditions where these enzymes behave as stable dimers, in the presence of 20% glycerol and 4 mg/ml BSA in the assay mixture (Table III). The corresponding Michaelis parameters were compared with those of the native, natural enzyme, the AspRS component from the multisynthetase complex purified from rat liver (33). The K_m value of each AspRS produced in yeast for $tRNA^{Asp}$ (0.5–0.6 μM) is identical to that of the complex-associated AspRS from rat (Table III). Similarly, the measured k_{cat} values are indistinguishable. Therefore, association of AspRS within the complex has no major influence on its catalytic activity.

Whereas the bacterial and yeast AspRS are very stable dimers, the monomer-dimer ratio can be easily modified in the case of the rat enzyme, by using mild experimental conditions (Table II). Glycerol stabilizes the dimeric form (Table II) as well as the enzymatic activity (Fig. 5). Decreasing glycerol concentration leads to rapid inactivation of AspRS-ΔN36 and, to a lesser extent, of AspRS-ΔN20 (Fig. 5). The presence of up to 20% glycerol is required to keep AspRS-ΔN36 or AspRS-ΔN20 fully active when incubated at 0.01 mg·ml^{-1} (~0.1 μM). In the presence of 5% or 0.5% glycerol, the half-life time of AspRS-ΔN36 is of 12 and 3 min, respectively. The full-length rAspRS is much less sensitive to the removal of glycerol in the incubation mixture. Its dissociation and inactivation requires the addition of chaotropic salts.

Upon incubation of rAspRS at 0.5 mg·ml^{-1} (4.4 μM) in the presence of 0.2 M KCl, dissociation occurs (Table II). The enzymatic activity of the sample decreases with a half-life time of about 80 min (Fig. 6). The residual activity is measured at 0 °C after dilution in the assay mixture containing 20% glycerol, to stabilize the remaining fraction of dimeric enzyme. In the case of rAspRS, when the assay was performed at 25 °C, a significant reactivation of AspRS was observed during the 10-min incubation in the assay mixture. When assayed at 0 °C, AspRS activity remains constant during this 10-min interval, and thus reflects the ratio of active and inactive forms in the sample after incubation in 0.2 M KCl at the times indicated. As shown in Fig. 6, the inactivation rate is dependent of the initial enzyme concentration. At protein concentrations of 0.44 and 0.06 μM, $t_{1/2}$ of rAspRS inactivation are of about 37 and 22 min, respectively. Amino acid activation and aminoacylation activities are lost at the same rate.

When the multisynthetase complex was incubated in the presence of 0.2 M KCl, its AspRS component (Cx-AspRS) inactivated, albeit less rapidly than rAspRS. Upon incubation of the complex at protein concentrations of 0.3 or 0.03 μM in conditions described in the legend of Fig. 6, the $t_{1/2}$ of Cx-AspRS inactivation was of about 40 min. Because Cx-AspRS remains tightly associated to the complex, the inactivation rate of Cx-AspRS was independent of the initial protein concentration in the incubation mixture.

When rAspRS is incubated at 20 °C, without KCl and in the presence of 5% glycerol, the enzyme is a dimer (Table II) and remains fully active even if incubated at low concentration (0.005 mg·ml^{-1}, ~0.04 μM) (Fig. 6). In the same conditions,

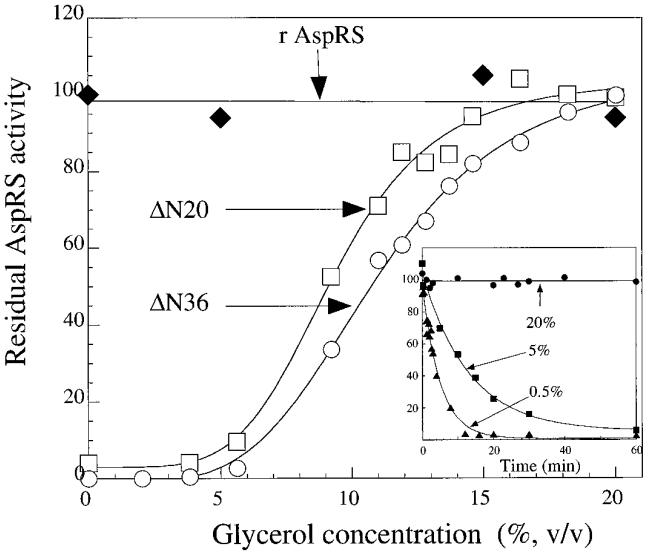

FIG. 5. **Dependence of the relative residual AspRS activity on the glycerol concentration.** The residual activities of rAspRS (♦), AspRS-ΔN20 (□), or AspRS-ΔN36 (○) incubated at 0.01 mg/ml (0.1 μM) for 30 min, at 4 °C, in 100 mM Tris-HCl, pH 7.5, 10 mM β-mercaptoethanol, containing BSA at 4 mg/ml and variable concentrations of glycerol, was measured in the $tRNA^{Asp}$ aminoacylation reaction immediately after dilution in the assay mixture containing 20% glycerol. The relative residual activity refers to the activity determined for each enzyme in the presence of 20% glycerol, prior to incubation in the buffer containing lower glycerol concentrations. *Inset*, time course of AspRS-ΔN36 inactivation after incubation as above, at 20 °C, in the presence of 20%, 5%, or 0.5% glycerol, as indicated.

AspRS-ΔN36 or AspRS-ΔN20 dissociates (Fig. 3 and Table II) and their enzymatic activity decreases rapidly, with a $t_{1/2}$ of inactivation of about 7 min (Fig. 6). The rate of enzyme inactivation decreased with increasing protein concentration, to give a $t_{1/2}$ of inactivation of ~20 min at 0.5 mg·ml^{-1} (4.5 μM). The substrates ATP or tRNA protect the enzyme against inactivation. In the presence of ATP (Fig. 6) or $tRNA^{Asp}$ in the incubation mixture, also containing 10 mM $MgCl_2$, AspRS-ΔN36 remains fully active, even when incubated at low concentration (~0.04 μM). A similar stabilizing effect was observed for rAspRS and AspRS-ΔN20. Addition of GTP instead of ATP has no stabilizing effect. The substrate ATP stabilizes the dimeric form of the enzyme. Upon chromatography of AspRS-ΔN20 on a Superose 12 column, as described in Fig. 3, in a buffer containing 5% glycerol, the enzyme behaves as a dimer or as a monomer, respectively, with or without the addition of 3 mM ATP and 10 mM $MgCl_2$ in the equilibration buffer.

The concentration-dependent inactivation rate observed above for the free, native or NH_2-terminal truncated forms of AspRS, cannot be explained if considering a simple monomer-dimer equilibrium, as shown in Reaction 1.

$$D \underset{k_{-1}}{\overset{k_1}{\rightleftarrows}} 2M$$

REACTION 1

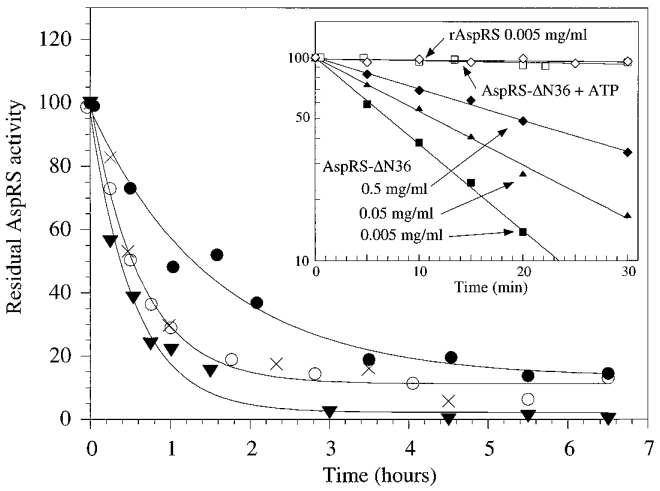

FIG. 6. **Concentration dependence of rAspRS and AspRS-ΔN36 inactivation.** The residual activity of rAspRS incubated at 0.5 mg/ml (4.4 μM; ●), 0.05 mg/ml (0.44 μM; ○, ×), or 0.007 mg/ml (0.06 μM; ▼) in 25 mM potassium phosphate, pH 7.5, 200 mM KCl, 10 mM DTE, at 0 °C, was measured in the $tRNA^{Asp}$ aminoacylation (●, ○, ▼) or [^{32}P]PP_i–ATP exchange (×) reactions. At the time intervals indicated, the dimer-monomer equilibrium was frozen by dilution at 0 °C in the assay mixture containing 20% glycerol and the assay was performed at 0 °C. The curves are simulated time courses using the rate constants given in the text. *Inset*, the residual aminoacylation activity of rAspRS (0.005 mg/ml; ◇), or of AspRS-ΔN36 incubated at 0.5 (♦), 0.05 (▲), or 0.005 (■, □) mg/ml in 100 mM Tris-HCl, pH 7.5, 10 mM β-mercaptoethanol, containing BSA at 4 mg/ml and 5% glycerol, with (□) or without (■) addition of 10 mM $MgCl_2$ and 3 mM ATP, at 20 °C, was determined as described above.

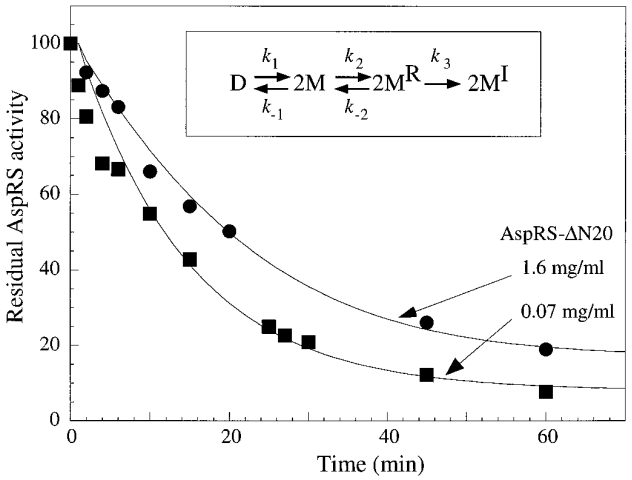

FIG. 7. **Time course of AspRS-ΔN20 inactivation and fitting of experimental data.** The residual activity of AspRS-ΔN20 incubated at 1.6 mg/ml (~15 μM; ●) or 0.07 mg/ml (~0.6 μM; ■) in 100 mM Tris-HCl, pH 7.5, 10 mM β-mercaptoethanol, containing BSA at 4 mg/ml and 5% glycerol, at 4 °C, was measured in the $tRNA^{Asp}$ aminoacylation reaction after dilution in the assay mixture containing 20% glycerol. The KINSIM program (35) was used to fit experimental data to the mechanism shown in the *inset*. The curves are simulated time courses using the rate constants given in the text.

Assuming that the dimer is the only active enzyme fraction, the time course of rAspRS inactivation (Fig. 6) can be satisfactorily fitted to the scheme shown by Reaction 2.

$$D \underset{k_{-1}}{\overset{k_1}{\rightleftarrows}} 2M \underset{k_{-2}}{\overset{k_2}{\rightleftarrows}} 2M^R$$

REACTION 2

M and M^R refer to monomeric species with or without the ability to dimerize, by using rate constants of $k_1 = 0.1\ min^{-1}$, $k_{-1} = 0.09\ \mu M^{-1}{\cdot}min^{-1}$, $k_2 = 0.05\ min^{-1}$, $k_{-2} = 0.0015\ min^{-1}$. Concerning the NH_2-terminal truncated AspRS species, the finding that large aggregates form upon incubation in dissociating buffers (Table II) suggests that the monomer is unstable and undergoes conformational changes that favor its aggregation. Accordingly, the simplest mechanism that can account for the experimental data is that shown in Reaction 3.

$$D \underset{k_{-1}}{\overset{k_1}{\rightleftarrows}} 2M \underset{k_{-2}}{\overset{k_2}{\rightleftarrows}} 2M^R \rightarrow 2M^I \rightarrow M^n$$

REACTION 3

M, M^R and M^I refer to the native, folded monomer (M) or to monomeric forms with reversible (M^R) or irreversible (M^I) conformational changes. M^I has a tendency to aggregate, leading to multimeric species (M^n). This mechanism of dissociation/inactivation of AspRS was tested in conditions where no aggregation occurs. Assuming that only D exhibits enzymatic activity, the time course of AspRS-ΔN20 inactivation (Fig. 7) can be satisfactorily fitted to this scheme by using rate constants of $k_1 = 0.07\ min^{-1}$, $k_{-1} = 0.39\ \mu M^{-1}{\cdot}min^{-1}$, $k_2 = 1.2\ min^{-1}$, $k_{-2} = 1\ min^{-1}$, and $k_3 = 10\ min^{-1}$. The rate-limiting step corresponds to dissociation of the enzyme. The removal of the NH_2-terminal extension generates a very unstable M^R species, leading to a monomer M^I, which is irreversibly inactivated. In the case of rAspRS, the rate constant k_3 is much lower and the dissociation/inactivation of the enzyme could be readily reversed, as shown below. The calculated theoretical curves shown in Figs. 6 and 7 are in good agreement with the experimental values. Therefore, the concentration dependence of AspRS inactivation is satisfactorily described if assuming that the only active enzyme species is the dimer. Consequently, reactivation of AspRS, requiring a process of bimolecular assembly, should conform to a second-order mechanism.

Dimerization of AspRS and Restoration of Enzyme Activity—Following incubation of rAspRS in an inactivation buffer containing 150 mM KCl, the time course of aspartylation was measured after dilution of at least 40-fold into the assay mixture. When the assay was performed at 25 °C, the amount of $Asp\text{-}tRNA^{Asp}$ formed did not increase linearly with the reaction time (Fig. 8*A*, □). This behavior contrasts with that observed when rAspRS is not incubated in the dissociation buffer prior to the assay (Fig. 8*A*, ■). The enhancement of the rate of $Asp\text{-}tRNA^{Asp}$ formation with the reaction time can be best explained if considering that reassociation of rAspRS occurs during the assay, and that the bimolecular reaction 2M → D is the rate-limiting step of the reactivation pathway. Accordingly, the initial rates of $Asp\text{-}tRNA^{Asp}$ formation increase by raising enzyme concentration in the assay (Fig. 8, *inset*). When the assay was performed at 0 °C (Fig. 8*B*), in conditions that do not assist the dimerization process, the increase of the reaction rate with time and the concentration dependence of the initial velocity curves, were no longer observed.

Such an enhancement of the aminoacylation rate with the reaction time was also detected when AspRS activity was assayed after incubation of the multisynthetase complex in the inactivation buffer (Fig. 8*A*, ○). It seems very unlikely that this effect could be due to a general structural perturbation of the complex. Indeed, formation of $Ile\text{-}tRNA^{Ile}$, catalyzed by the IleRS component, a monomeric enzyme (36), varied linearly with the reaction time (Fig. 8*A*, ◇). As in the case of rAspRS, a linear time-course of $Asp\text{-}tRNA^{Asp}$ formation was observed when the reaction is conducted at 0 °C (Fig. 8*B*); no reactivation/reassociation of Cx-AspRS occurred during the assay. The kinetic behaviors of rAspRS and Cx-AspRS are very similar, indicating that in both cases, enzyme inactivation/reactivation

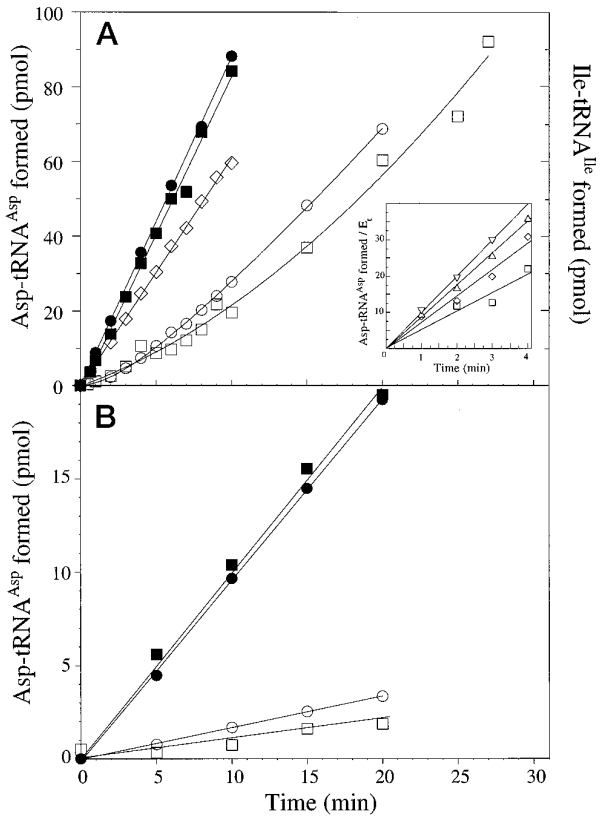

FIG. 8. **Concentration dependence of AspRS reactivation.** The purified enzyme preparations, rAspRS at 0.009 mg/ml (80 nM) and the rat multisynthetase complex at 0.1 mg/ml (~70 nM; 1 mol of the dimeric Cx-AspRS and of the monomeric Cx-IleRS components per mol of complex), were incubated at 4 °C, for 18 h, in a stabilizing buffer containing 50 mM potassium phosphate, pH 7.5, 2 mM DTE, 20% glycerol, and BSA at 4 mg/ml (*closed symbols*), or in a dissociating buffer containing 50 mM Tris-HCl, pH 7.5, 150 mM KCl, 2 mM DTE, and BSA at 4 mg/ml (*open symbols*). *A*, the time course of the tRNA^{Asp} (■, □, ●, ○) or tRNA^{Ile} (◇) aminoacylation reaction catalyzed by the residual enzyme fractions of rAspRS (■, □), Cx-AspRS (●, ○), and Cx-IleRS (◇) was determined at 25 °C, after dilution in 100 mM Tris-HCl pH 7.5, 2 mM DTE, 4 mg/ml BSA. Enzyme concentrations in the assay are of about 2 nM. *Inset*, dependence of the initial rates of Asp-tRNA^{Asp} formation on rAspRS concentration in the assay mixture. rAspRS was incubated in the dissociation buffer as described above, and the formation of Asp-tRNA^{Asp} was followed in the presence of various rAspRS concentrations in the assay mixture: 1 (□), 2 (◇), 4 (△), or 8 (▽) nM. Results are expressed in moles of Asp-tRNA^{Asp} formed/mol of enzyme (E_t) as a function of time. *B*, the time course of the tRNA^{Asp} aminoacylation reaction catalyzed by the residual rAspRS (■, □) or Cx-AspRS (●, ○) enzyme fractions was determined at 0 °C after appropriate dilution in the assay mixture containing 10% glycerol. Enzyme concentrations in the assay are of about 4 nM.

correlates with dissociation/reassociation of a dimeric AspRS. However, the initial rate of Asp-tRNA^{Asp} formation, catalyzed at 25 °C or 0 °C by Cx-AspRS previously incubated in dissociating conditions, increases linearly with the enzyme concentration (in the range of 2–60 nM). As already mentioned above, Cx-AspRS is not released from the complex after incubation in the presence of 0.2 M KCl. Therefore, association of two AspRS monomers, which remain bound to the complex, is an intramolecular process, and reactivation follows an apparent first-order mechanism independent of enzyme concentration.

DISCUSSION

The NH_2-terminal extension of rat AspRS, as well as its association within a multienzyme complex, are dispensable *in vitro* for the catalytic activity, as assessed by the determination of the Michaelis parameters for the complex-associated, the free native recombinant, and the free NH_2-terminal truncated forms, which proved to be indistinguishable. This study provides additional evidence for the concept that eukaryotic synthetases possess additional autonomous domains not found in their prokaryotic counterparts, and endowed with a functional role unrelated to catalysis. The facultative character of those extra-domains was reported for other eukaryotic AspRS (23, 37), as well as for other synthetases from yeast or mammals (38–43).

The ability of rat AspRS to dissociate under nondenaturing conditions provided a suitable tool to study the structure/function relationships for an AspRS species. The dissociation of rat AspRS and the concomitant loss of both amino acid activation and tRNA aminoacylation activities establish for the first time that dimerization of AspRS, a representative of class IIb synthetases, is absolutely required for its catalytic activity. Our results are in agreement with those previously reported for a class IIa synthetase, Pro-tRNA synthetase from *E. coli*, where dimerization has also been shown to be required for activity (44). Therefore, oligomerization seems to be a key element for enzyme activity catalyzed by class II aminoacyl-tRNA synthetases with an α_2-type structure, although the two active sites of AspRS simultaneously bind ATP or the analog AMP-PCP (4). In addition, two tRNA^{Asp} molecules are bound per dimeric enzyme, each tRNA molecule involving a single monomer (45). This situation contrasts with that observed for a class IIa dimeric enzyme, Pro-RNA synthetase from *T. thermophilus* (46), where the variable arm and the TΨC loop of a tRNA molecule bind to one monomer, whereas aminoacylation of that tRNA molecule is performed into the active site of the other monomer. In that particular case, structural data provide a rational explanation for the absolute requirement of dimerization for activity.

Monomeric species of bacterial and yeast AspRS have not been obtained so far in nondenaturing conditions (37, 47), and a strict relationship between activity and the α_2 conformation could not be established. However, experimental evidence supporting the structural importance of dimerization of yeast AspRS on the conformation of its active site has been reported (13). Mutation of the conserved Pro^{273} residue of motif 1, located at the dimeric interface, impaired the catalytic activity of the enzyme but did not abolish dimerization. The catalytic capacity of a mutant subunit was found to be restored into heterodimers formed by association of a mutant subunit with a wild-type subunit. The effect of dimerization was interpreted in terms of a structural constraint that helps to fold the two active sites into an active conformation, in a cooperative manner. Accordingly, structural data reveal that the two active sites are closely related, through a network of hydrogen bonds and salt bridges involving the side chains of several residues from motifs 1, 2, and 3 of both subunits. Although these residues are located at the dimeric interface, especially those from motif 1, several observations suggest that they do not have a pre-eminent role in the stabilization of the α_2 dimers. (i) Well conserved motifs 1, 2, and 3 have been unambiguously identified in two class II enzymes, eukaryotic Ala-tRNA synthetase and yeast mitochondrial Phe-tRNA synthetase, which are functional monomers (15, 16). (ii) A mutation in motif 1 lowered the activity of the enzyme but did not affect its dimerization capacity (13). (iii) In this study, we have shown that rat AspRS displays a dimer dissociation constant at least 1 order of magnitude above that of the yeast enzyme, although their motifs 1 are very similar (17). The NH_2-terminal truncated derivatives are very unstable dimers. It is therefore very likely that the NH_2-terminal extension of the eukaryotic enzymes plays a major role in the stabilization of active dimers. These extensions are absent from the prokaryotic AspRS. In that case, the

stability of the dimeric interface is contributed by an additional COOH-terminal domain (17). The possibility to easily monitor the dimer/monomer equilibrium provided the opportunity to correlate the activity of AspRS and its oligomeric state and led to the identification of an intimate connection between the formation of the dimer and the emergence of a productive conformation of the active site. (i) Dissociation of the dimer correlates with the loss of amino acid activation and tRNA aminoacylation activities. (ii) In the presence of ATP, the inactivation rate is much slower and the two subunits remain associated. These results suggest that the productive conformation of the active site requires structural rearrangements that are induced by dimerization, and correlatively that the presence of ATP in the active site stabilizes its productive conformation and therefore stabilizes the dimeric conformation of the enzyme. Accordingly, one would expect that the two active sites are functionally related. The finding that a Lys-tRNA synthetase mutant affected in its dimeric interface displays cooperativity toward lysine binding strongly supports this hypothesis (14).

The crystal structure of *T. thermophilus* and *S. cerevisiae* AspRS provided a detailed description of the dimeric interface (17). In addition to residues from the three conserved motifs of class II synthetases, which are highly conserved in all known AspRS species, interchain interactions involve four major contact areas: the long helix H3 and strand A1 from the beginning of the COOH-terminal catalytic domain, a four-stranded antiparallel β-sheet involving strands I1 and I2 from the two monomers, helix H2b from the hinge region of one monomer that interacts with helices H4 and H11 from the catalytic domain of the other subunit, and the NH_2-terminal anticodon-binding domain of one monomer and the catalytic domain of the other. Because of the close homology between the various AspRS species in these regions, a rational explanation for the lesser stability of the mammalian enzyme awaits accurate structural investigations. The availability of large amounts of purified rat AspRS opens the way for crystallization studies. However, one may already speculate that the NH_2-terminal polypeptide extension that characterizes all the eukaryotic AspRS species, whose structural arrangement could not be defined in the crystal structure of the yeast enzyme, might be implicated in the stabilization of the α_2 dimer, through direct contacts with the other subunit or through the stabilization of the NH_2-terminal anticodon binding domain of one subunit into a conformation that favors its interaction with the catalytic domain of the other subunit.

Acknowledgments—We are indebted to J. Rossier and J.-P. Le Caer for the protein sequence analyses, to G. Batelier for performing the analytical ultracentrifuge experiments, to D. Moras for the gift of a sample of yeast AspRS, and to D. Pompon for the pYeDP60 vector. We gratefully acknowledge the excellent technical assistance of M.-T. Latreille during part of this work.

REFERENCES

1. Schimmel, P., and Söll, D. (1979) *Annu. Rev. Biochem.* **48,** 601–648
2. Eriani, G., Delarue, M., Poch, O., Gangloff, J., and Moras, D. (1990) *Nature* **347,** 203–206
3. Cavarelli, J., and Moras, D. (1993) *FASEB J.* **7,** 79–86
4. Cavarelli, J., Eriani, G., Rees, B., Ruff, M., Boeglin, M., Mitschler, A., Martin, F., Gangloff, J., Thierry, J.-C., and Moras, D. (1994) *EMBO J.* **13,** 327–337
5. Belrhali, H., Yaremchuk, A., Tukalo, M., Larsen, K., Berthet-Colominas, C., Leberman, R., Beijer, B., Sproat, B., Als-Nielsen, J., Grübel, G., Legrand, J.-F., Lehmann, M., and Cusack, S. (1994) *Science* **263,** 1432–1436
6. Onesti, S., Miller, A. D., and Brick, P. (1995) *Structure* (*London*) **3,** 163–176
7. Mosyak, L., Reshetnikova, L., Goldgur, Y., Delarue, M., and Saffro, M. G. (1995) *Nat. Struct. Biol.* **2,** 537–547
8. Arnez, J. G., Harris, D. C., Mitschler, A., Rees, B., Francklyn, C. S., and Moras, D. (1995) *EMBO J.* **14,** 4143–4155
9. Logan, D. T., Mazauric, M.-H., Kern, D., and Moras, D. (1995) *EMBO J.* **14,** 4156–4167
10. Madern, D., Anselme, J., and Härtlein, M. (1992) *FEBS Lett.* **299,** 85–89
11. Davis, M. W., Buechter, D. D., and Schimmel, P. (1994) *Biochemistry* **33,** 9904–9911
12. Lu, Y., and Hill, K. A. W. (1994) *J. Biol. Chem.* **269,** 12137–12141
13. Eriani, G., Cavarelli, J., Martin, F., Dirheimer, G., Moras, D., and Gangloff, J. (1993) *Proc. Natl. Acad. Sci. U. S. A.* **90,** 10816–10820
14. Commans, S., Blanquet, S., and Plateau, P. (1995) *Biochemistry* **34,** 8180–8189
15. Ripmaster, T. L., Shiba, K., and Schimmel, P. (1995) *Proc. Natl. Acad. Sci. U. S. A.* **92,** 4932–4936
16. Sanni, A., Walter, P., Boulanger, Y., Ebel, J.-P., and Fasiolo, F. (1991) *Proc. Natl. Acad. Sci. U. S. A.* **88,** 8387–8391
17. Delarue, M., Poterszman, A., Nikonov, S., Garber, M., Moras, D., and Thierry, J. C. (1994) *EMBO J.* **13,** 3219–3229
18. Mirande, M. (1991) *Prog. Nucleic Acid Res. Mol. Biol.* **40,** 95–142
19. Mirande, M., and Waller, J.-P. (1989) *J. Biol. Chem.* **264,** 842–847
20. Jacobo-Molina, A., Peterson, R., and Yang, D. C. H. (1989) *J. Biol. Chem.* **264,** 16608–16612
21. Reed, V. S., and Yang, D. C. H. (1994) *J. Biol. Chem.* **269,** 32937–32941
22. Mirande, M., Lazard, M., Martinez, R., and Latreille, M.-T. (1992) *Eur. J. Biochem.* **203,** 459–466
23. Escalante, C., and Yang, D. C. H. (1993) *J. Biol. Chem.* **268,** 6014–6023
24. Urban, P., Cullin, C., and Pompon, D. (1990) *Biochimie* (*Paris*) **72,** 463–472
25. Sambrook, J., Fritsch, E. F., and Maniatis, T. (1989) *Molecular Cloning: A Laboratory Manual*, 2nd Ed., Cold Spring Harbor Laboratory, Cold Spring Harbor, NY
26. Sanger, F., Nicklen, S., and Coulson, A. R. (1977) *Proc. Natl. Acad. Sci. U. S. A.* **74,** 5463–5467
27. Ito, N., Fukuda, Y., Murata, K., and Kimura, A. (1993) *J. Bacteriol.* **153,** 163–168
28. Gornall, A. G., Bardawill, C. J., and David, M. M. (1949) *J. Biol. Chem.* **177,** 751–766
29. Kellermann, O., Brevet, A., Tonetti, H., and Waller, J.-P. (1979) *Eur. J. Biochem.* **99,** 541–550
30. Laemmli, U. K. (1970) *Nature* **227,** 680–685
31. Laue, T. M., Shah, B. D., Ridgeway, T. M., and Pelletier, S. L. (1992) in *Analytical Ultracentrifugation in Biochemistry and Polymer Science* (Harding, S. E., Rowe, A. J., and Horton, J. C., eds) pp. 90–125, Royal Society of Chemistry, Cambridge, United Kingdom
32. Romanos, M. A., Scorer, C. A., and Clare, J. J. (1992) *Yeast* **8,** 423–488
33. Cirakoglu, B., and Waller, J.-P. (1985) *Biochim. Biophys. Acta* **829,** 173–179
34. Huang, S., Elliott, R. C., Liu, P.-S., Koduri, R. K., Weickmann, J. L., Lee, J.-H., Blair, L. C., Ghosh-Dastidar, P., Bradshaw, R. A., Bryan, K. M., Einarson, B., Kendall, R. L., Kolacz, K. H., and Saito, K. (1987) *Biochemistry* **26,** 8242–8246
35. Barshop, B. A., Wrenn, R. F., and Frieden, C. (1983) *Anal. Biochem.* **130,** 134–145
36. Lazard, M., Mirande, M., and Waller, J.-P. (1985) *Biochemistry* **24,** 5099–5106
37. Eriani, G., Prevost, G., Kern, D., Vincendon, P., Dirheimer, G., and Gangloff, J. (1991) *Eur. J. Biochem.* **200,** 337–343
38. Cirakoglu, B., and Waller, J.-P. (1985) *Eur. J. Biochem.* **151,** 101–110
39. Vellekamp, G., Sihag, R. K., and Deutscher, M. P. (1985) *J. Biol. Chem.* **260,** 9843–9847
40. Walter, P., Weygand-Durasevic, I., Sanni, A., Ebel, J.-P., and Fasiolo, F. (1989) *J. Biol. Chem.* **264,** 17126–17130
41. Martinez, R., and Mirande, M. (1992) *Eur. J. Biochem.* **207,** 1–11
42. Ludmerer, S. W., Wright, D. J., and Schimmel, P. (1993) *J. Biol. Chem.* **268,** 5519–5523
43. Bec, G., Kerjan, P., and Waller, J.-P. (1994) *J. Biol. Chem.* **269,** 2086–2092
44. Lee, M.-L., and Muench, K. H. (1969) *J. Biol. Chem.* **244,** 223–230
45. Cavarelli, J., Rees, B., Ruff, M., Thierry, J.-C., and Moras, D. (1993) *Nature* **362,** 181–184
46. Biou, V., Yaremchuk, A., Tukalo, M., and Cusack, S. (1994) *Science* **263,** 1404–1410
47. Eriani, G., Dirheimer, G., and Gangloff, J. (1990) *Nucleic Acids Res.* **18,** 7109–7118